An image plate chamber for x-ray diffraction experiments in Debye–Scherrer geometry

Oliver Stachs[a] and Thomas Gerber
Universität Rostock, Fachbereich Physik, Universitätsplatz 3, 18051 Rostock, Germany

Valeri Petkov
Department of Physics and Astronomy, Michigan State University, East Lansing, Michigan 48824-1116

(Received 24 September 1999; accepted for publication 11 August 2000)

A new design for implementation of x-ray diffraction experiments is proposed. The exploitation of the imaging plate technique opens new possibilities to carry out diffraction experiments. The detector chamber in Debye–Scherrer geometry equipped with an image plate takes advantage of this technology such as high resolution, high sensitivity, linearity in intensity, and linearity over the detector area. The proof of this measurement principle is demonstrated by presentation of the x-ray diffraction pattern of corundum (crystalline), nickel (crystalline), and sodium borate (amorphous). © *2000 American Institute of Physics.* [S0034-6748(00)03611-X]

I. INTRODUCTION

The x-ray diffraction technique is a useful instrument for investigation and characterization of the solid state. That a diversity of experimental technique may be profitably employed is a direct consequence of the wide range of state of order and crystalline structure. Thus the apparatus that is best suited to obtain a specific kind of information about the sample, e.g., crystal structure, degree of crystallinity, size of crystalline regions, or mode of preferred orientation, may be quite different from that suited to another goal. In the past diffraction procedures have been classified into two types according to whether the pattern has been recorded photographically or by means of an electronic counter (direct recording of the diffracted intensities). The imaging plate technique with x-ray storage phosphors opens the possibility to incorporate the advantages of both. The registration simultaneously offers the following advantages: the x-ray source does not have to be highly stable and the entire diffraction pattern can be inspected at once. X-ray storage phosphors ($BaFX:Eu^{2+}$, X=Cl, Br) have been studied extensively because they exhibit photostimulated luminescence (PSL) and offer an alternative to conventional x-ray imaging technology.[1–4]

The principal disadvantage of the old photographic technique, that the intensities cannot be determined with highest quantitative accuracy, is not present. An inspection of the entire diffraction pattern may supply the answer to many questions: crystalline or amorphous, two or three dimensional ordering, preferred orientation, etc. Further evaluation of the diffraction pattern preserved with the imaging plate reveals the possibility of carrying out linear slices in a different direction or a radial integration.

[a]Author to whom correspondence should be addressed; electronic mail: oliver.stachs@med.uni-rostock.de

II. INSTRUMENT DESCRIPTION

A scheme of the instrument is shown in Fig. 1. The chamber is constructed in analogy to a conventional Debye–Scherrer camera for different collimation conditions (point or line collimation). X rays from the source pass through slit system and Kapton foil and are diffracted by the sample. The first slit system consists of a horizontal and a vertical slit in combination with a second vertical slit for elimination of the slit and Kapton foil scattering to minimize background scattering (Figs. 2 and 3). This slit system offers a high flexibility in the beam geometry depending on the experimental requirements (pinehole, line focus). The sample is placed in the center of the Θ–2Θ circle in symmetrical transmission geometry mounted on an adjustable sample holder (see Fig. 3). Specimens that are composed randomly oriented (crystalline or amorphous) can be mounted with a simple technique since there is no texture in the sample. For Debye–Scherrer cameras the specimens should be cylinders of about 1 mm diameter or less, depending on the mass absorption coefficient. These cylindrical samples may be prepared by filling a capillary with the sample powder, by mechanical cutting, molding the bulk into cylindrical shape, or by building up a sheet of many thin fibers and trimming it to a cylindrical cross section. A pattern of fibers with axial orientation are mostly prepared with the fibers axis normal to the incident x-ray beam. The direction on the plate parallel to the fiber axis is the *meridian* and the direction at the right angle is the *equator*.

The unscattered beam leaves the chamber through a second Kapton window without contact with the imaging plate or any part of the second slit. The imaging plate[5,6] is placed on the wall of the chamber at a distance of 90 mm from the center of the Θ–2Θ circle. The aluminum chamber can be evacuated by means of a diffusion pump to minimize background scattering and for sample protection. Note, that is important to shield the environment of the primary beam in front of the chamber to minimize the parasitic scattering.

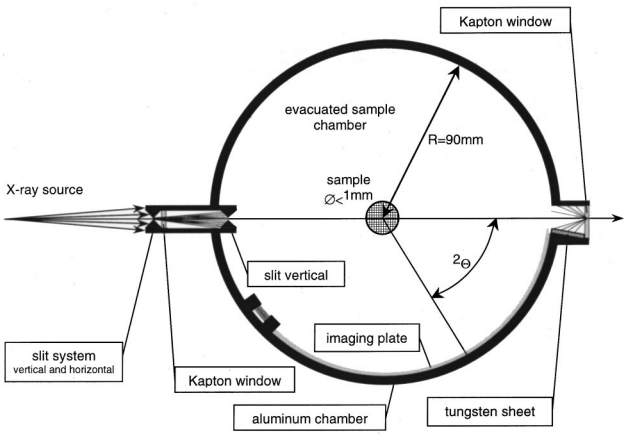

FIG. 1. Schematic layout of the detector system (top view). The principle of the imaging plate chamber is shown. For demonstration, the parasitic scattering of the slit system and the Kapton foil are depicted explicitly.

The storage phosphor imaging technology offers several advantages over traditional detection methods such as x-ray films and proportional counters. For example, storage phosphors are 10–100 times more sensitive to incident radiation than x-ray films, having a linear dynamic range over 5 magnitudes and a spatial resolution up to 25 μm. Performance details are given in Refs. 7–10. For the measurements Fujifilm imaging plates BAS-IP SR 2025 20×25 cm in combination with a BAS 5000 phoshor imaging system from Fuji Medical Systems were used for exposure. This system has a theoretical scan resolution of 25 μm, a digital resolution of 16 bit, and a dynamic range of 5 orders of magnitude.[11,12] The imaging plate chamber can be equipped with different sizes of imaging plates and in one or two equatorial directions. Using the BAS-IP SR 2025 a maximal scattering angle $2\Theta=160°$ is applicable.

FIG. 2. The detector chamber mounted on a conventional x-ray tube at the Michigan State University. The chamber is hinged on a Huber goniometer for adjustment.

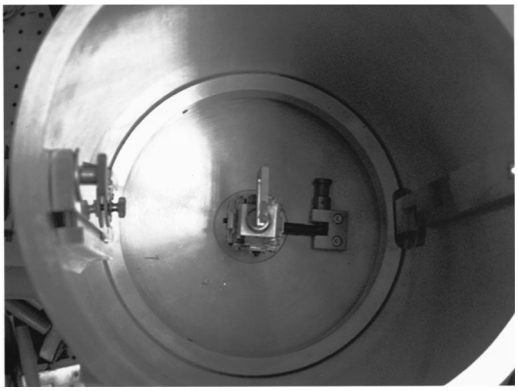

FIG. 3. View of the inside of the chamber with sample holder and support for imaging plate.

III. APPLICATIONS

A two dimensional x-ray pattern obtained from polycrystalline corundum is shown in Fig. 4. The pattern was recorded with a rotating anode in microfocus mode (0.1×1 mm) using Ag K_α radiation ($\lambda=0.560\,87$ Å) with a high voltage of 45 keV and current of 12 mA. The x-ray diffraction experiments were carry out using a graphite monochromator with the size of admittance slits of 0.1×1 mm. The exposure time was 1 h. The imaging plate was read with 16 bit digital resolution and a resolution of 25 μm. In consideration of the chamber geometry and wavelength these values indicate a theoretical resolution of 4×10^{-4} deg in 2Θ.

The Debye–Scherrer rings are elliptical due to the cylindrical geometry of the chamber. For geometrical correction cylindrical coordinates have to be implemented. This is essential for a radial integration. The integral intensity of linear slice with a width of 3 mm in equatorial direction is

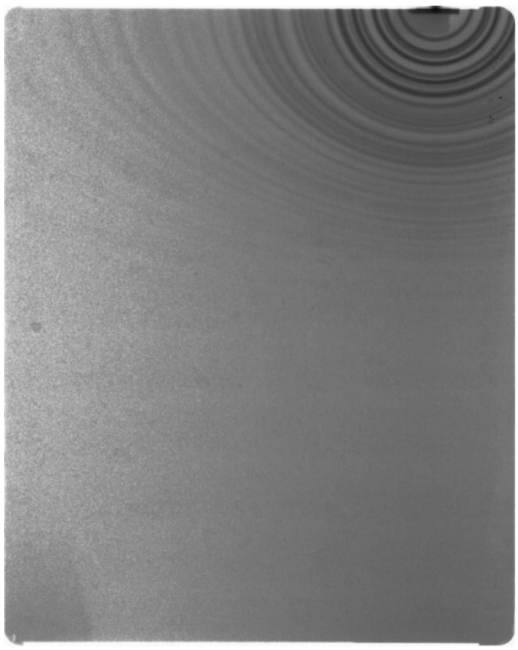

FIG. 4. The two dimensional diffraction pattern obtained from polycrystalline corundum. The Debye–Scherrer rings are elliptical due to cylindrical geometry of the chamber.

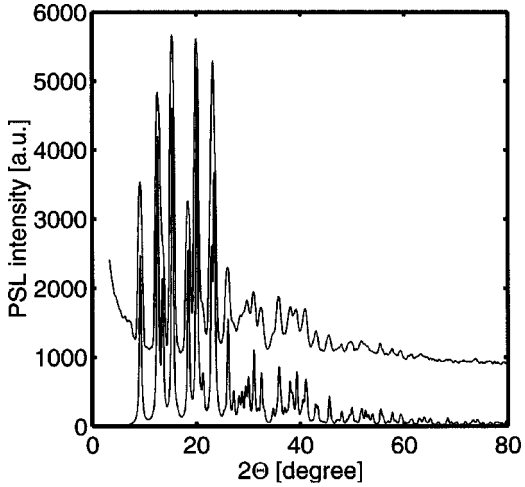

FIG. 5. Observed (top) and calculated (bottom) x-ray diffraction profile for polycrystalline corundum obtained from a 3 mm equatorial slice in Fig. 4 (PSL). The peak width of the observed curve is caused by the crystallite size of the specimen.

shown in Fig. 5. In comparison, the theoretical intensity distribution for corundum, calculated with a peak breadth at full width at half maximum of 0.5°, is depicted. The experimental intensity was not corrected for background in order to show the low parasitic scattering.

For demonstration Fig. 6 shows the diffraction spectrum from an amorphous sodium borate sample. The diffraction pattern was detected under the same conditions mentioned above. The intensity distribution was calculated from a 2 mm slice in the equatorial direction.

Figure 7 clarifies the high potential and the eventually occurring background problems of the detector system. As shown, the diffraction pattern of nickel powder is filled in a 0.5 mm capillary for the diffraction experiments. The pattern was recorded at the beamline 1-ID at SRICAT (Advanced Photon Source, Argonne National Laboratory) in focused mode (point focus) in air. The energy of 65 keV enabled a

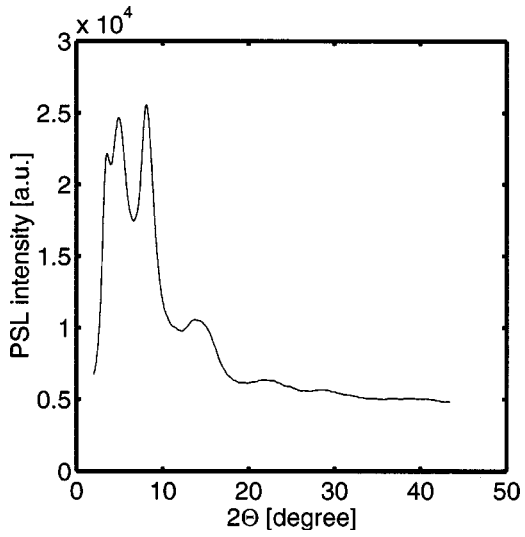

FIG. 6. Observed and background corrected x-ray diffraction profile for corundum sodium borate (PSL).

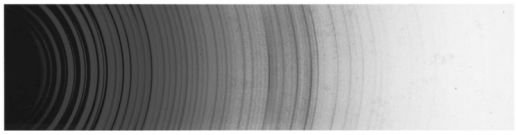

FIG. 7. Two dimensional diffraction pattern obtained from crystalline nickel powder recorded at beamline 1-lD at SRICAT (Advanced Photon Source, Argonne National Laboratory) with 65 keV and 15 s exposure time.

maximal theoretical scattering vector of 65 $Å^{-1}$. The very short exposure time of 15 s shows the high efficiency. Beyond, the pattern clarifies the rise of the air scattering around the primary beam in the sample chamber, unless evacuated. Furthermore, a shadow in the lower and the left part of the pattern caused by shielding can be seen. These two facts show that it is very important to shield the flypath and to evacuate the sample chamber.

IV. RESULTS

We present an imaging plate chamber for x-ray scattering experiments in Debye–Scherrer geometry. The detector chamber is a simple and transportable detector system for conventional x-ray tubes and synchrotron radiation, which takes advantage of the high performance of the imaging plate technique. The exploitation of the image plate as an area detector opens the possibility of investigation of specimens with orientations.

The geometry of the chamber results in a low background scattering. The integrated slit system offers high flexibility in the beam geometry depending on the experimental requirements. The imaging plate system can be advanced with a high pressure cell, temperature cell, or cooling stage. One drawback is that it is not possible to integrate an energy filter in the diffracted beam. More information and details about construction will be available.[13]

ACKNOWLEDGMENTS

The authors thank Falk Tofaute for technical assistance. This study was supported by BMBF (Grant No. 03Ge4ROK-4) and Deutsche Akademie der Naturforscher Leopoldina funded by BMBF.

[1] J. Miyahara, K. Takahashi, Y. Amemiya, N. Kamiya, and Y. Satow, Nucl. Instrum. Methods Phys. Res. A **246**, 572 (1986).
[2] M. Sonoda, M. Takano, J. Miyahara, and H. Kato, Radiology **148**, 833 (1983).
[3] K. Takahashi, J. Miyahara, and Y. Shibahara, J. Electrochem. Soc. **132**, 1492 (1985).
[4] K. Takahashi, K. Kohda, J. Miyahara, Y. Kanemitsu, K. Amitani, and S. Shionoya, J. Lumin. **31/32**, 266 (1984).
[5] J. Miyahara, Chemistry Today **223**, 29 (1989).
[6] Y. Amemiya and J. Miyahara, Nature (London) **336**, 89 (1988).
[7] M. Thomas, H. von Seggern, and A. Winnacker, Phys. Rev. B **17**, 9240 (1991).
[8] M. Sonoda, M. Takano, J. Miyahara, and H. Kato, Radiology **148**, 833 (1983).
[9] M. Thoms, Nucl. Instrum. Methods Phys. Res. A **389**, 437 (1997).
[10] Y. Kudo, S. Kojima, K.-Y. Liu, S. Kowado, T. Ishikawa, and K. Hirano, Rev. Sci. Instrum. **66**, 4487 (1995).
[11] W. Hillen, U. Schiebel, and T. Zaengel, Med. Phys. **14**, 744 (1987).
[12] J. Miyahara, K. Takahashi, Y. Amemiya, N. Kamiya, and Y. Satow, Nucl. Instrum. Methods Phys. Res. A **246**, 572 (1986).
[13] oliver.stachs@med.uni-rostock.de